Available online at www.sciencedirect.com
SCIENCE DIRECT
Journal of Sound and Vibration 296 (2006) 1–22
JOURNAL OF SOUND AND VIBRATION
www.elsevier.com/locate/jsvi

Semi-active control of three-dimensional vibrations of an inclined sag cable with magnetorheological dampers

Q. Zhou[a,b,*], S.R.K. Nielsen[a], W.L. Qu[b]

[a]*Department of Civil Engineering, Aalborg University, Sohngaardsholmsvej 57, DK-9000 Aalborg, Denmark*
[b]*Hubei Key Laboratory of Roadway Bridge and Structure Engineering, Wuhan University of Technology, Wuhan 430070, PR China*

Received 16 March 2005; received in revised form 15 July 2005; accepted 31 October 2005
Available online 17 April 2006

Abstract

Three-dimensional semi-active vibration control of an inclined sag cable with discrete magnetorheological (MR) dampers is investigated in this paper using the finite difference method (FDM). A modified Dahl model is used to describe the dynamic property of MR damper. The nonlinear equations of motion of cable–dampers system are first established, which accounts for coupling between in-plane and out-of-plane motions, and also for the displacement of the support points. A MR damper can be considered as a variable friction damper approximately, so a semi-active control strategy based on the modulated homogeneous friction algorithm is proposed. Taking a typical short cable as an example, the vibration reduction ability with optimally controlled MR dampers is verified numerically by comparison with the viscous damper tuned to a single mode response. The analysis show that, if the conditions are fulfilled at which the optimal tuned viscous damper is designed, the MR damper and the viscous damper are performing equally well; however, if the response of the cable is dominated by several modes, the MR damper can achieve better vibration reduction effect compared with viscous damper. Especially, if the amplitude of the support point motion less than a threshold value, MR damper can prevent subharmonic excitation caused by support point motion from taking place, consequently, MR damper achieves significant vibration reduction compared to viscous damper. In addition, the influence of measurement noise on control effect and the robustness of the proposed semi-active control rule are also examined.

1. Introduction

Due to large flexibility, relatively small mass and extremely low inherent damping, cables used in bridges and to support masts and towers may be prone to excessive vibrations, either caused by wind or a combination of wind and rain, or by the motion of the supported structures, which can cause premature cable or connection failure and consequently reduce the service life of the cable structure [1]. To overcome cable vibration problems transversally attached passive dampers have been implemented in various bridges for vibration mitigation. Kovacs found that the maximum modal damping ratio that could be provided by the damper was approximately half the relative distance of the damper from the support [2]. Pacheo et al. [3] introduced

*Corresponding author. Hubei Key Laboratory of Roadway Bridge and Structure Engineering, Wuhan University of Technology, Wuhan 430070, PR China. Tel.: +86 27 87160361; fax: +86 27 87160361.
E-mail address: drzhouqiang@hotmail.com (Q. Zhou).

0022-460X/$ - see front matter © 2006 Elsevier Ltd. All rights reserved.
doi:10.1016/j.jsv.2005.10.028

nondimensional parameter to develop a "universal estimation curve" for the linear viscous damper. Yu and Xu [4] developed a hybrid method to study three-dimensional vibration of inclined cable with oil dampers and to consider the influence of cable sag, cable inclination and damper direction and others. Krenk [5] performed a complex modal analysis for a taut cable with viscous damper and obtained an accurate explicit asymptotic solution for the damping properties in terms of the complex wavenumber. Krenk and Nielsen [6] extended the complex modal analysis to cables with sag, and obtained explicit results for the modal damping ratios and for the optimal tuning of the damper. Further, Nielsen and Krenk [7] studied the whirling harmonic motion around the chord line of a shallow cable with viscous damper caused by nonlinear coupling of pairs of modes. Main and Jones [8] studied free vibration of a taut cable with a linear viscous damper and obtained the range of attainable modal damping ratios and corresponding oscillation frequencies in every mode for a given damper location without approximation. However, the optimal damping ratio for linear damper can be achieved in only one mode of vibration: if the damper is designed for optimal performance in a particular mode, it will be too rigid in higher modes and too compliant in lower modes. So some other types of damping devices have been investigated as alternatives to the linear damper for cable vibration reduction. Carne [9] investigated a friction damper using equivalent energy dissipation criterion. Kovacs et al. [10] made a similar numerical analysis of this damper. The free vibration of a taut cable with a nonlinear power-law damper was investigated by Main and Jones [11]. They derived an approximate analytical solution for the amplitude-dependent effective damping ratios in each mode, and pointed out that nonlinear damper could potentially allow optimal damping performance to be achieved over a wider range of modes than in the linear case. Besides, theoretical and experimental studies of active control of cable vibrations by axial support motion and active tension control have also been explored [12–15]. However, a number of implementation difficulties remain to be solved before fully active vibration control becomes practically applicable in bridge cables.

Recently, research attention has been paid to semi-active control of cable vibration. Semi-active dampers can offer the adaptability of active control devices without requiring the associated large power sources, and moreover, semi-active dampers are fail-safe since they can serve as passive dampers if the power fails. Johnson et al. [16] demonstrated that smart semi-active damping could provide 50–80% reduction in cable response compared with the optimal passive linear damper. It should be noted that only the ideal semi-active damper is used in Johnson's study, so, the indicated significant reduction can hardly be achieved in reality. However, the study suggests that smart damper could be an effective replacement for passive viscous damping of cables. One semi-active device that appears to be particularly promising is the magnetorheological (MR) damper. Ni et al. [17] developed neural network control strategies corresponding to a full-order system model and a reduced-order modal model for semi-active vibration control of stay cables using MR dampers. Through a series of numerical studies of the benchmark cable-stayed bridge problem, Moon et al. [18] investigated the effectiveness of the SMC-based semi-active control system using the MR dampers in mitigating structural responses for a wide range of seismic loading conditions. The implementation of MR dampers to a cable-stayed bridge and field measurements showed that the MR dampers could effectively mitigate cable vibration caused by wind-and-rain excitation or other excitation sources [19,20].

The three-dimensional semi-active vibration control of an inclined sag cable with MR dampers is investigated in this paper. The three-dimensional problem is studied because dampers usually are installed in pairs to stay cables to keep the damper system stable and to reduce both in-plane and out-of-plane cable vibration simultaneously [4]. At first, the nonlinear equations of motion of the cable–damper system are established, taking the cable sag, cable inclination, flexural rigidity of the cable, damper direction and others parameters into consideration. The derived governing equations account for coupling between in-plane and out-of-plane motions, and also for the displacement of the support points. Among the various numerical methods applied to cable dynamics, the finite difference method (FDM) and the finite element method (FEM) are commonly used [21–24]. In this paper, the FDM is adopted. After the field equations have been discretized, the Newmark beta integration method incorporated with the Newton–Raphson iteration technique is used to solve resulting nonlinear governing ordinary differential equations. The semi-active control strategy based on the modulated homogeneous friction algorithm is proposed. Because only the local dynamic response, i.e., the displacement and velocity of the MR dampers are measured, and moreover, the structural parameters of the cable cannot be accurate, the proposed control rule is robust and to be readily implemented. Taking a typical short cable as an example, the vibration reduction ability with MR dampers is verified numerically by

comparison with the optimal viscous damper. The influence of measurement noise on control effect and the robustness of the proposed semi-active control rule are also examined.

2. Mechanics of damper and cable

2.1. Mechanical model of MR damper

It is very important to establish an accurate mechanical model of the MR damper in order to simulate the damper property and structural vibration control properly. Up to now, the phenomenological model based on the Bouc-Wen model proposed by Spencer et al. [25] is rather accurate to describe dynamical behaviour of MR damper. However, the number of parameters to be identified is up to 14, which lead to some problems in practical applications. Essentially, MR damper can be considered as a variable friction damper. However, the well-known Coulomb model cannot capture the velocity–force relationship of the MR damper when the velocity is near zero [25], so it is rational that some hysteresis models described to friction force are adopted to simulate the mechanical property of MR damper. Recently, according to experimental results, Zhou and Qu [26] suggested a more simple and effective modified Dahl model as shown in Fig. 1. In this model, the Dahl hysteresis model instead of the Bouc-Wen model is adopted to simulate Coulomb force to avoid the determination of too many parameters. Besides, the modified Dahl model can well capture the force–velocity relationship in the low velocity region.

The damper force is given by

$$F = K_0 x + C_0 \dot{x} + F_d Z - f_0, \tag{1}$$

where K_0 is stiffness, C_0 is damping coefficient, F_d is Coulomb force modulated by applied magnetic field, x is displacement of MR damper, f_0 is damper force caused by seals and measurement bias. Z is nondimensional hysteretic variable governed by [27]

$$\dot{Z} = \sigma \dot{x}(1 - Z\,\mathrm{sgn}(\dot{x})), \tag{2}$$

where σ determines hysteretic loop shape.

In order to calibrate the modified Dahl model under an applied fluctuating magnetic field, it is necessary to obtain relationship between model parameters and applied magnetic field. The experimental results show that C_0 and F_d are related with applied voltage as follows:

$$C_0 = C_{0s} + C_{0d} u, \quad F_d = F_{ds} + F_{dd} u, \tag{3}$$

where C_{0s} and F_{ds} are damping coefficient and Coulomb force of MR damper at 0 V, respectively. u is an intrinsic variable to determine the function dependence of the parameters on the applied voltage V. The relationship between u and V is modelled by the first-order filter [25],

$$\dot{u} = -\eta(u - V), \tag{4}$$

where η reflect response time of MR damper, namely, larger η means shorter response time. V is applied voltage.

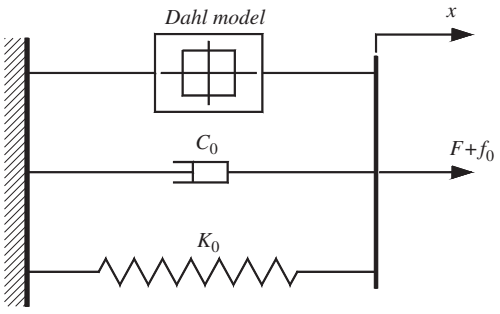

Fig. 1. Modified Dahl model of MR damper.

Therefore, a total of eight parameters (C_{0s}, C_{0d}, F_{ds}, F_{dd}, K_0, σ, f_0 and η) should be determined for the proposed MR damper model.

In order to verify the proposed modified Dahl model, a MR damper was produced and the corresponding experiment was carried out. Figs. 2 and 3 are the comparison between the experimental results and the theoretical results when the voltage applied to the MR damper is constant and changeable, respectively. The agreement shows that the modified Dahl model can simulate the dynamic characteristics of the MR damper with sufficient accuracy.

2.2. Equations of motion of cable

This study concerns three-dimensional vibration of an inclined sag cable with MR dampers installed near the cable supporting points as shown in Fig. 4. The cable is assumed to be shallow; for a horizontal cable, this requires the sag-to-span ratio ranging from nearly zero to about 1:8; for inclined cables the assumption presumes a somewhat smaller range of sag [28]. The model of the cable is written in a local coordinate system as indicated in Fig. 4. The local x coordinate is taken along the chord line while the y coordinate is in the gravity plane orthogonal to the chord line. The cable is assumed to have a uniform cross section along its length. Considering the flexural rigidity of the cable, the nonlinear equations of motion of the cable with MR dampers can be expressed as

$$\frac{\partial}{\partial s}\left[(T+\tau)\left(\frac{\mathrm{d}x}{\mathrm{d}s}+\frac{\partial u}{\partial s}\right)\right]+F_x+\sum_{j=1}^{M}F_{\mathrm{d}x,j}\delta(s-s_j)=m\frac{\partial^2 u}{\partial t^2}-mg\sin\theta+c_1\frac{\partial u}{\partial t}, \tag{5}$$

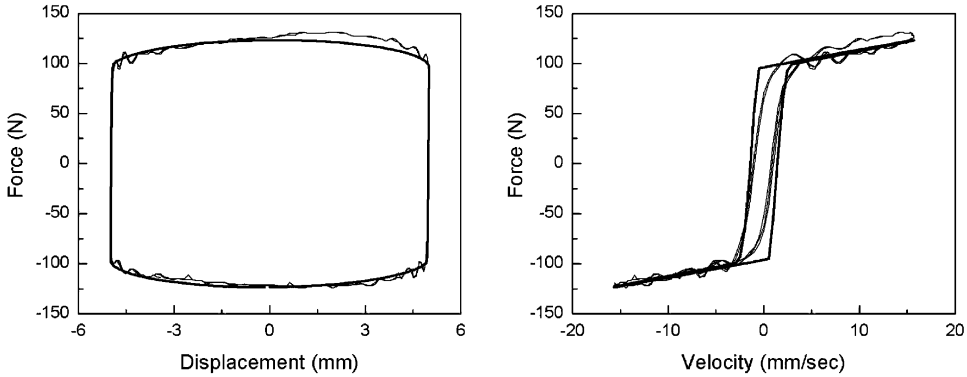

Fig. 2. Verification of the proposed modified Dahl model when applied voltage is constant: thick line, analytical result; thin line, experimental result.

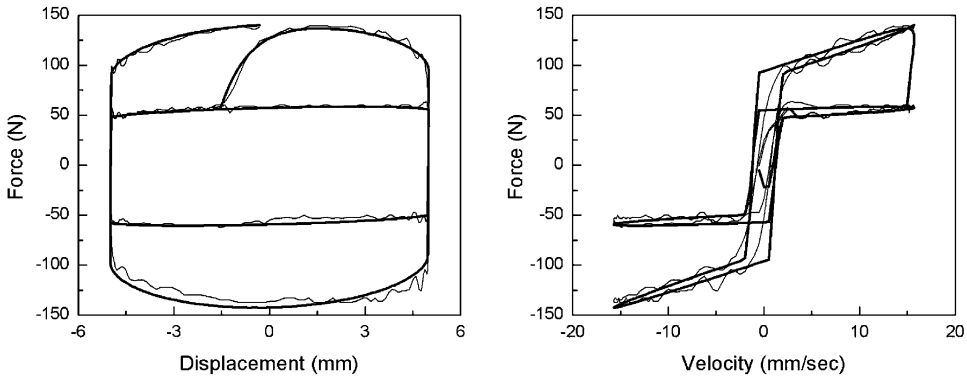

Fig. 3. Verification of the proposed modified Dahl model when applied voltage is fluctuated: thick line, analytical result; thin line, experimental result.

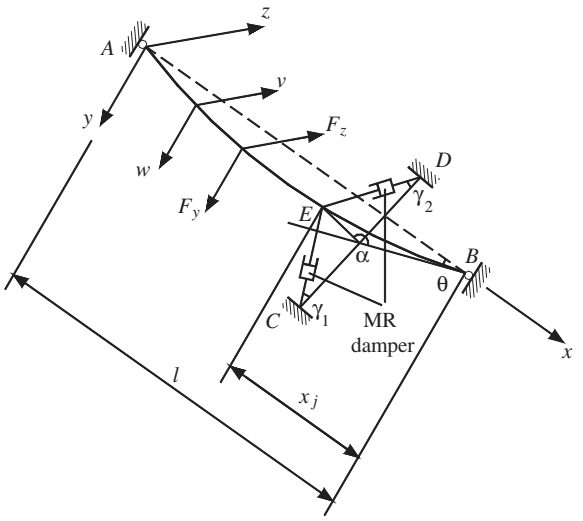

Fig. 4. Schematic diagram of an inclined sag cable with MR dampers.

$$-EI\frac{\partial^4(y+w)}{\partial x^4}+\frac{\partial}{\partial s}\left[(T+\tau)\left(\frac{\mathrm{d}y}{\mathrm{d}s}+\frac{\partial w}{\partial s}\right)\right]+F_y+\sum_{j=1}^{M}F_{\mathrm{d}y,j}\delta(s-s_j)=m\frac{\partial^2 w}{\partial t^2}-mg\cos\theta+c_1\frac{\partial w}{\partial t}, \tag{6}$$

$$-EI\frac{\partial^4 v}{\partial x^4}+\frac{\partial}{\partial s}\left[(T+\tau)\frac{\partial v}{\partial s}\right]+F_z+\sum_{j=1}^{M}F_{\mathrm{d}z,j}\delta(s-s_j)=m\frac{\partial^2 v}{\partial t^2}+c_2\frac{\partial v}{\partial t}, \tag{7}$$

where T is the static cable tension; τ is the additional dynamic cable tension; u, w and v are the cable dynamic displacement components in the x, y and z direction, respectively, measured from the static equilibrium position; s is the Lagrangian coordinate in the unstrained cable profile; F_x, F_y and F_z are external dynamic loading per unit length in the x, y and z direction, respectively; $F_{\mathrm{d}x,j}$, $F_{\mathrm{d}y,j}$ and $F_{\mathrm{d}z,j}$ are the forces generated by the jth MR damper on the cable at the location of s_j in the x, y and z direction, respectively; E is Young's modulus of the cable material; I is moment of inertia of cable cross section; M is the total number of MR dampers; δ is the Dirac's delta function; m is the mass of the cable per unit length; t is the time; θ is the angle of chord line with respect to the horizontal plane; c_1 and c_2 are the in-plane and out-of-plane internal damping coefficients of the cable, respectively; and g is the acceleration due to gravity.

Introduce the following transformations:

$$\frac{\partial}{\partial s}=\frac{1}{\sqrt{1+y_x^2}}\frac{\partial}{\partial x},\quad H=T\frac{\mathrm{d}x}{\mathrm{d}s},\quad h=\tau\frac{\mathrm{d}x}{\mathrm{d}s}. \tag{8}$$

Because the profile is shallow, the longitudinal component of the equation of motion is considered unimportant, and is dropped [28]. Considering the equations of static equilibrium of the cable, Eqs. (6) and (7) can be rewritten as

$$-EI\frac{\partial^4(y+w)}{\partial x^4}+\frac{1}{\sqrt{1+y_x^2}}\frac{\partial}{\partial x}\left[(H+h)\frac{\partial w}{\partial x}+hy_x\right]+F_y+\sum_{j=1}^{M}F_{\mathrm{d}y,j}\delta(x-(l-x_j))=m\frac{\partial^2 w}{\partial t^2}+c_1\frac{\partial w}{\partial t}, \tag{9}$$

$$-EI\frac{\partial^4 v}{\partial x^4}+\frac{1}{\sqrt{1+y_x^2}}\frac{\partial}{\partial x}\left[(H+h)\frac{\partial v}{\partial x}\right]+F_z+\sum_{j=1}^{M}F_{\mathrm{d}z,j}\delta(x-(l-x_j))=m\frac{\partial^2 v}{\partial t^2}+c_2\frac{\partial v}{\partial t}, \tag{10}$$

where H and h are the components of the static cable tension and dynamic cable tension in the x direction, respectively; y_x is the first derivative of y with respect to x; x_j is the coordinate of the jth MR damper; and l is the cable chord length.

Within the shallow cable approximation the static curve of the cable is the parabola

$$y = \frac{mgl^2 \cos\theta}{2H}\frac{x}{l}\left[1 - \left(\frac{x}{l}\right)\right]. \tag{11}$$

The additional dynamic cable tension can be assumed constant along the cable span [29] and can be expressed as [28]

$$h\left(\frac{\mathrm{d}s}{\mathrm{d}x}\right)^3 = EA\left[\frac{\partial u}{\partial x} + \frac{\mathrm{d}y}{\mathrm{d}x}\frac{\partial w}{\partial x} + \frac{1}{2}\left(\frac{\partial w}{\partial x}\right)^2 + \frac{1}{2}\left(\frac{\partial v}{\partial x}\right)^2\right], \tag{12}$$

where A is cross-sectional area of cable.

The boundary conditions of the cable considered here are:

$$u(0,t) = u_1(t), \quad u(l,t) = u_2(t), \tag{13a}$$

$$w(0,t) = w_1(t), \quad w(l,t) = w_2(t), \tag{13b}$$

$$v(0,t) = v_1(t), \quad v(l,t) = v_2(t). \tag{13c}$$

Then the three components of displacement u, w and v can be expressed in the form

$$u(x,t) = u_s(x,t), \quad w(x,t) = w_s(x,t) + w_d(x,t), \quad v(x,t) = v_s(x,t) + v_d(x,t), \tag{14}$$

where $u_s(x,t)$, $w_s(x,t)$ and $v_s(x,t)$ are the pseudo-static displacements in the x, y and z direction, respectively; and $w_d(x,t)$ and $v_d(x,t)$ are the relative dynamic displacements in the y and z direction, respectively.

From the geometry of a cable under different support motion [30], the pseudo-static displacement are given by [31]

$$u_s(x,t) = \left(1 - \frac{x}{l}\right)u_1(t) + \frac{x}{l}u_2(t), \tag{15a}$$

$$w_s(x,t) = \left(1 - \frac{x}{l}\right)w_1(t) + \frac{x}{l}w_2(t), \tag{15b}$$

$$v_s(x,t) = \left(1 - \frac{x}{l}\right)v_1(t) + \frac{x}{l}v_2(t). \tag{15c}$$

Substituting Eq. (15) into Eqs. (9) and (10), and omitting $c_1[(\partial w_s(x,t))/\partial t]$ and $c_2[(\partial v_s(x,t))/\partial t]$, then Eqs. (9) and (10) can be rewritten as

$$\begin{aligned} &-EI\frac{\partial^4 w_d}{\partial x^4} + \frac{1}{\sqrt{1+y_x^2}}\frac{\partial}{\partial x}\left[(H+h)\frac{\partial w_d}{\partial x} + hy_x\right] + F_y + \sum_{j=1}^{M} F_{\mathrm{d}y,j}\delta(x-(l-x_j)) \\ &\quad = m\frac{\partial^2 w_d}{\partial t^2} + c_1\frac{\partial w_d}{\partial t} + m\frac{\partial^2 w_s}{\partial t^2}, \end{aligned} \tag{16}$$

$$-EI\frac{\partial^4 v_d}{\partial x^4} + \frac{1}{\sqrt{1+y_x^2}}\frac{\partial}{\partial x}\left[(H+h)\frac{\partial v_d}{\partial x}\right] + F_z + \sum_{j=1}^{M} F_{\mathrm{d}z,j}\delta(x-(l-x_j)) = m\frac{\partial^2 v_d}{\partial t^2} + c_2\frac{\partial v_d}{\partial t} + m\frac{\partial^2 v_d}{\partial t^2}. \tag{17}$$

Substituting Eqs. (8), (11), (14), (15) into Eq. (12), performing the integration over l and discarding the differentials of high orders result in

$$\frac{hL_e}{EA} = (u_2 - u_1) + \frac{mg\cos\theta}{H}\int_0^l w_d\,\mathrm{d}x + \frac{1}{2}\int_0^l \left(\frac{\mathrm{d}w_d}{\mathrm{d}x}\right)^2 \mathrm{d}x + \frac{1}{2}\int_0^l \left(\frac{\mathrm{d}v_d}{\mathrm{d}x}\right)^2 \mathrm{d}x, \tag{18}$$

where L_e denotes the so-called effective cable length

$$L_e = \int_0^l \left(\frac{\mathrm{d}s}{\mathrm{d}x}\right)^3 \mathrm{d}x \approx \int_0^l \left(1 + \frac{3}{2}\left(\frac{\mathrm{d}y}{\mathrm{d}x}\right)^2\right)\mathrm{d}x = l\left[1 + 8\left(\frac{f}{l}\right)^2\right], \tag{19}$$

where f is the sag at mid-span

$$f = \frac{mgl^2 \cos\theta}{8H}. \tag{20}$$

From Eq. (18), one can notice that h depends on both w_d and v_d. Therefore, Eqs. (16) and (17) account for coupling between in-plane and out-of-plane motions.

2.3. Damper forces

Let us consider the force $F_{dy,j}$ and $F_{dz,j}$ produced by the jth MR damper on the cable in the y and z direction, respectively. The direction of each damper from the deck to the cable is defined as the positive direction.

The displacement and velocity of the MR damper linking the points C and E are, see Fig. 4,

$$[X_C \;\; \dot{X}_C] = [\cos\alpha\sin\gamma_1 \;\; -\sin\alpha\sin\gamma_1 \;\; \cos\gamma_1] \begin{bmatrix} -\sin\theta & 0 \\ \cos\theta & 0 \\ 0 & 1 \end{bmatrix} \begin{bmatrix} w_d(l-x_j,t) & \dot{w}_d(l-x_j,t) \\ v_d(l-x_j,t) & \dot{v}_d(l-x_j,t) \end{bmatrix}, \tag{21}$$

where α and γ_1 are defined in Fig. 4.

After the displacement and velocity of the MR damper are known, the output force $F_{d,C}$ can easily be obtained from Eqs. (1) and (2). Then, the two components of $F_{d,C}$ in the y and z directions are given by

$$\begin{Bmatrix} F_{dy,C} \\ F_{dz,C} \end{Bmatrix} = \begin{bmatrix} -\sin\theta & \cos\theta & 0 \\ 0 & 0 & 1 \end{bmatrix} \begin{Bmatrix} -\cos\alpha\sin\gamma_1 \\ \sin\alpha\sin\gamma_1 \\ -\cos\gamma_1 \end{Bmatrix} F_{d,C}. \tag{22}$$

Similarly, For the MR damper linking points D and E, see Fig. 4, the displacement and velocity become

$$[X_D \;\; \dot{X}_D] = [\cos\alpha\sin\gamma_2 \;\; -\sin\alpha\sin\gamma_2 \;\; -\cos\gamma_2] \begin{bmatrix} -\sin\theta & 0 \\ \cos\theta & 0 \\ 0 & 1 \end{bmatrix} \begin{bmatrix} w_d(l-x_j,t) & \dot{w}_d(l-x_j,t) \\ v_d(l-x_j,t) & \dot{v}_d(l-x_j,t) \end{bmatrix}. \tag{23}$$

The two components of $F_{d,D}$ in the y and z directions are given by

$$\begin{Bmatrix} F_{dy,D} \\ F_{dz,D} \end{Bmatrix} = \begin{bmatrix} -\sin\theta & \cos\theta & 0 \\ 0 & 0 & 1 \end{bmatrix} \begin{Bmatrix} -\cos\alpha\sin\gamma_2 \\ \sin\alpha\sin\gamma_2 \\ \cos\gamma_2 \end{Bmatrix} F_{d,D}. \tag{24}$$

2.4. Discretization of differential equation

The FDM is applied to discretize the nonlinear partial differential Eqs. (16) and (17). The cable length is divided into $(n+1)$ equidistance nodes with $x_0 = 0$ and $x_{n+1} = l$. The interval distance between the ith and $(i+1)$th nodes is $a = l/(n+1)$. Using the central difference algorithm, the derivatives of the dynamic displacement component at the ith node can be expressed as

$$\left(\frac{\partial^2 w_d}{\partial x^2}\right)_i = \frac{1}{a^2}(w_{d,i+1} - 2w_{d,i} + w_{d,i-1}), \tag{25a}$$

$$\left(\frac{\partial^4 w_d}{\partial x^4}\right)_i = \frac{1}{a^4}(w_{d,i+2} - 4w_{d,i+1} + 6w_{d,i} - 4w_{d,i-1} + w_{d,i-2}), \tag{25b}$$

$$\left(\frac{\partial^2 v_d}{\partial x^2}\right)_i = \frac{1}{a^2}(v_{d,i+1} - 2v_{d,i} + v_{d,i-1}), \tag{25c}$$

$$\left(\frac{\partial^4 v_d}{\partial x^4}\right)_i = \frac{1}{a^4}(v_{d,i+2} - 4v_{d,i+1} + 6v_{d,i} - 4v_{d,i-1} + v_{d,i-2}). \tag{25d}$$

By integration by part, follows

$$\int_0^l \left(\frac{\mathrm{d}w_d}{\mathrm{d}x}\right)^2 \mathrm{d}x = -\int_0^l w_d \frac{\mathrm{d}^2 w_d}{\mathrm{d}x^2}\,\mathrm{d}x. \tag{26}$$

Then, the last two terms of the right-hand side of Eq. (18) can be given as

$$\frac{1}{2}\int_0^l \left(\frac{\mathrm{d}w_d}{\mathrm{d}x}\right)^2 = -\frac{1}{2}a\sum_{j=1}^{n} w_{d,j}\left(\frac{\mathrm{d}^2 w_d}{\mathrm{d}x^2}\right)_j = \frac{1}{a}\left[\sum_{j=1}^{n} w_{d,j}^2 - \sum_{j=1}^{n-1} w_{d,j}w_{d,j+1}\right], \tag{27a}$$

$$\frac{1}{2}\int_0^l \left(\frac{\mathrm{d}v_d}{\mathrm{d}x}\right)^2 = -\frac{1}{2}a\sum_{j=1}^{n} v_{d,j}\left(\frac{\mathrm{d}^2 v_d}{\mathrm{d}x^2}\right)_j = \frac{1}{a}\left[\sum_{j=1}^{n} v_{d,j}^2 - \sum_{j=1}^{n-1} v_{d,j}v_{d,j+1}\right]. \tag{27b}$$

Substituting Eqs. (25) and (27) into Eqs. (16)–(18) yields the following ordinary differential equations:

$$\begin{aligned} &m\ddot{w}_{d,i} + c_1\dot{w}_{d,i} + \frac{Hl^2}{\psi^2 a^4}(w_{d,i+2} - 4w_{d,i+1} + 6w_{d,i} - 4w_{d,i-1} + w_{d,i-2}) + f_{1,i} - \sum_{j=1}^{n} F_{\mathrm{d}y,j}(x - (l - x_j)) \\ &+ \frac{1}{\sqrt{1 + y_{x,i}^2}}\left[H + \frac{EA}{L_e}(u_2 - u_1)\right]\frac{1}{a^2}(w_{d,i+1} - 2w_{d,i} + w_{d,i-1}) + \frac{1}{\sqrt{1 + y_{x,i}^2}}\frac{\lambda^2 H}{l^3}a\sum_{j=1}^{n} w_{d,j} \\ &= F_y - m\frac{\partial^2 w_s}{\partial t^2} - \frac{1}{\sqrt{1 + y_{x,i}^2}}\frac{mg\cos\theta}{H}\frac{EA}{L_e}(u_2 - u_1), \end{aligned} \tag{28}$$

$$\begin{aligned} &m\ddot{v}_{d,i} + c_1\dot{v}_{d,i} + \frac{Hl^2}{\psi^2 a^4}(v_{d,i+2} - 4v_{d,i+1} + 6v_{d,i} - 4v_{d,i-1} + v_{d,i-2}) + f_{2,i} - \sum_{j=1}^{n} F_{\mathrm{d}z,j}(x - (l - x_j)) \\ &+ \frac{1}{\sqrt{1 + y_{x,i}^2}}\left[H + \frac{EA}{L_e}(u_2 - u_1)\right]\frac{1}{a^2}(v_{d,i+1} - 2v_{d,i} + v_{d,i-1}) = F_z - m\frac{\partial^2 v_s}{\partial t^2}, \end{aligned} \tag{29}$$

where $f_{1,i}$ and $f_{2,i}$ are nonlinear terms given as

$$\begin{aligned} f_{1,i} = &-\frac{1}{\sqrt{1 + y_{x,i}^2}}\frac{EA}{aL_e}\frac{mg\cos\theta}{H}(w_{d,i+1} - 2w_{d,i} + w_{d,i-1})\sum_{j=1}^{n} w_{d,j} \\ &-\frac{1}{\sqrt{1 + y_{x,i}^2}}\frac{EA}{a^3 L_e}(w_{d,i+1} - 2w_{d,i} + w_{d,i-1})\left[\left[\sum_{j=1}^{n} w_{d,j}^2 - \sum_{j=1}^{n-1} w_{d,j}w_{d,j+1}\right] + \left[\sum_{j=1}^{n} v_{d,j}^2 - \sum_{j=1}^{n-1} v_{d,j}v_{d,j+1}\right]\right] \\ &+\frac{1}{\sqrt{1 + y_{x,i}^2}}\frac{EA}{aL_e}\frac{mg\cos\theta}{H}\left[\left[\sum_{j=1}^{n} w_{d,j}^2 - \sum_{j=1}^{n-1} w_{d,j}w_{d,j+1}\right] + \left[\sum_{j=1}^{n} v_{d,j}^2 - \sum_{j=1}^{n-1} v_{d,j}v_{d,j+1}\right]\right], \end{aligned} \tag{30}$$

$$\begin{aligned} f_{2,i} = &-\frac{1}{\sqrt{1 + y_{x,i}^2}}\frac{EA}{aL_e}\frac{mg\cos\theta}{H}(v_{d,i+1} - 2v_{d,i} + v_{d,i-1})\sum_{j=1}^{n} w_{d,j} \\ &-\frac{1}{\sqrt{1 + y_{x,i}^2}}\frac{EA}{a^3 L_e}(v_{d,i+1} - 2v_{d,i} + v_{d,i-1})\left[\left[\sum_{j=1}^{n} w_{d,j}^2 - \sum_{j=1}^{n-1} w_{d,j}w_{d,j+1}\right] + \left[\sum_{j=1}^{n} v_{d,j}^2 - \sum_{j=1}^{n-1} v_{d,j}v_{d,j+1}\right]\right]. \end{aligned} \tag{31}$$

λ^2 is the nondimensional Irvine parameter for sag extensibility given as [28]

$$\lambda^2 = \left(\frac{mgl\cos\theta}{H}\right)^2 l\,\frac{EA}{HL_e} \tag{32}$$

and parameter ψ, which indicates the relative importance of cable and beam action, is defined as [28]

$$\psi = L\sqrt{\frac{H}{EI}}. \tag{33}$$

When ψ is small, it indicates that beam action predominates. While ψ is large, cable action is of primary importance.

The nonlinear equations of dynamic equilibrium (28) and (29) are solved by an incremental-iterative algorithm based on the Newmark beta algorithm in combination to Newton–Raphson iteration [32].

3. Control strategies

Essentially, MR damper can be considered as a variable friction damper. Inaudi proposed a control strategy for the design of semi-active friction controllers, the so-called modulated homogeneous friction algorithm [33], which can obtain quadratic dissipation of energy per cycle in the deformation amplitude and maximum dissipation efficiency for resistance-force level proportional to deformation. In this control algorithm, the control friction force for the ith MR damper is proportional to the absolute value of the previous local peak of the damper deformation signal, that is,

$$N_i = \beta_i \left| P[X_i(t)] \right|, \tag{34}$$

where $\beta_i > 0$ is controller gain, $P[X_i(t)]$ is local peak of the displacement of the MR damper prior to the current time t, and can be defined as

$$P[X_i(t)] = X_i(t-s), \quad s = \left\{ \min \bar{t} \geqslant 0 : \frac{\mathrm{d}X_i(t-\bar{t})}{\mathrm{d}t} = 0 \right\}, \tag{35}$$

where s is time interval between the immediate previous local peak and the current time t. After N_i is obtained, and if η is large enough, from Eq. (4) it can be assumed that u is approximately equal to V, so according to Eq. (3b), the required voltage for MR damper is given by

$$V_{i,\mathrm{need}} = \frac{N_i - F_{ds,i}}{F_{dd,i}}. \tag{36}$$

As a semi-active controller, the applied voltage to MR damper has a range from 0 to $V_{\max}$. So the semi-active control strategy can take on the following form:

$$V_i = \begin{cases} 0 & V_{i,\mathrm{need}} < 0, \\ V_{i,\mathrm{need}} & 0 \leqslant V_{i,\mathrm{need}} \leqslant V_{\max}, \\ V_{\max} & V_{i,\mathrm{need}} > V_{\max}. \end{cases} \tag{37}$$

From Eq. (34), it should be noticed that the implementation of the control strategy requires only the measurements of displacement and velocity of the MR dampers.

Compared with other control algorithms based on optimal control theory [34], such as the linear quadratic regular algorithm, and instantaneous optimal control algorithm, the proposed semi-active control algorithm has some advantages. The most important merit is the easy implementation because only the local dynamic responses (displacement and velocity) of the MR dampers are required, and the structural parameters of cable–dampers system can be estimated roughly. However, the controller gain should be properly determined only through numerical parameter studies numerical for a given structure. It should be noted that the proposed semi-active control strategy ignores any information that might be available if some observers are used.

4. Numerical simulations

A typical short cable is selected for detailed studies. The chord length L is 144.08 m, the modulus of elasticity E is 1.95×10^{11} Pa, the equilibrium force H is 1.32×10^{7} N, the cross-sectional area A is 0.0314 m^2, the moment of inertia I is 7.854×10^{-5} m^4, the cable mass per unit length m is 260.62 kg/m, and inclination θ is 37.2°. The two main parameters of the cable, i.e. λ^2 and ψ, are 0.2287 and 133.8, respectively.

The cable natural frequencies of in-plane and out-of-plane modes of the inclined cable without dampers are given in Table 1. The primary critical damping ξ of in-plane and out-of-plane vibration of cable is assumed the same and equal to 0.1%, and the corresponding damping constant of in-plane and out-of-plane vibration c_1 and c_2 is obtained by [35]

$$c_1 = c_2 = 2\xi\sqrt{EAm}. \tag{38}$$

To achieve the possible maximum reduction of dynamic response of cable in both in-plane and out-of-plane vibrations, a pair of MR dampers are installed symmetrically to the cable at a position x_j of 3.33% L with damper direction $\gamma_1 = \gamma_2 = 45°$ and $\alpha = 52.8°$. The angle α is chosen in a way that the damper forces are acting normal to the chord line of the inclined cable, which can be regarded as optimum direction [36]. The parameters of the MR damper are listed in Table 2, and the adjustable voltage range is from 0 to 7 V.

To demonstrate the vibration reduction effect with MR dampers, the dynamic response analysis with an optimal viscous damper is also performed. The installation pattern of viscous dampers is the same as that of MR dampers. If the flexural rigidity of the cable is ignored, then the optimal normalized damper size $c/(mL\omega_1)(x_j/L)$ for the first mode is about 0.10 [3,5]. However, in this study, because of the influence of flexural rigidity, the optimal normalized damper size increases to 0.13, i.e., the optimum damping coefficient C_{opt} is taken as 7.2536×10^5 N s/m, as shown in Fig. 5.

After extensive numerical analysis, it can be found that there exists an optimal controller gain β in semi-active control rule (more detail can be seen in Section 4.4). For the given short cable, the optimal gain β is about 5.0×10^6, which is selected in the following analysis.

The cable is divided into 30, 60 and 90 elements, respectively, and correspondingly the displacement responses of the cable with MR dampers subjected to external force and to support point motion are shown in Fig. 6. It can be seen that when $n = 29$, i.e., the cable is divided into 30 elements, the calculation results is accurate enough.

4.1. In the case of external force

At first the dynamic response of cable with dampers subjected to a uniformly distributed zero-mean, stationary Guassian random load. The random load is acting normal to the chord line of the inclined cable as shown in Fig. 7. The auto-spectral density function of the process is chosen as bandlimited white noise with a central frequency of 2.5 Hz, and a bandwidth of 5.0 Hz, which cover the first six in-plane and out-of-plane modes of the cable. The peak value of the applied load is 350 N/m, acting under 45° to the XY plane,

Table 1
Natural frequencies of in-plane and out-of-plane modes of cable

Mode order	Natural frequency (Hz)		Remark
	In-plane	Out-of-plane	
1	0.788	0.781	Symmetric mode
2	1.562	1.562	Antisymmetric mode
3	2.343	2.343	Symmetric mode
4	3.124	3.124	Antisymmetric mode
5	3.905	3.905	Symmetric mode
6	4.686	4.686	Antisymmetric mode

Table 2
Parameter of MR damper

C_{0s} (N s/m)	C_{0d} (N s/m/V)	F_{ds} (N)	F_{dd} (N/V)	K_0 (N/m)	σ (m^{-1})	f_0 (N)	η (s^{-1})
2.4×10^4	3.6×10^3	2.0×10^3	1.5×10^4	3.0×10^4	5.0×10^4	0.0	200

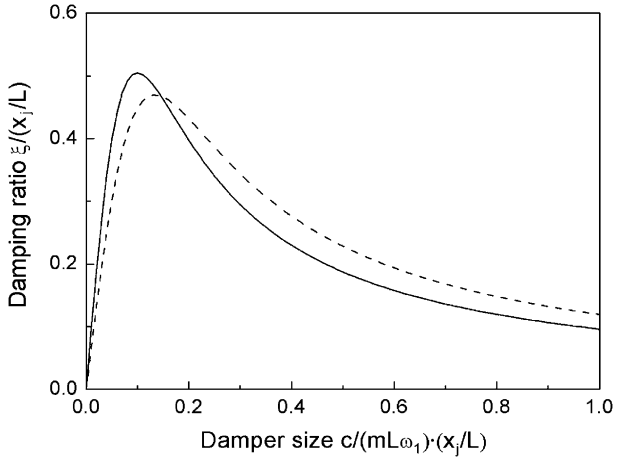

Fig. 5. Damping ratio of the first mode: solid line, EI is ignored; dashed line, EI is considered.

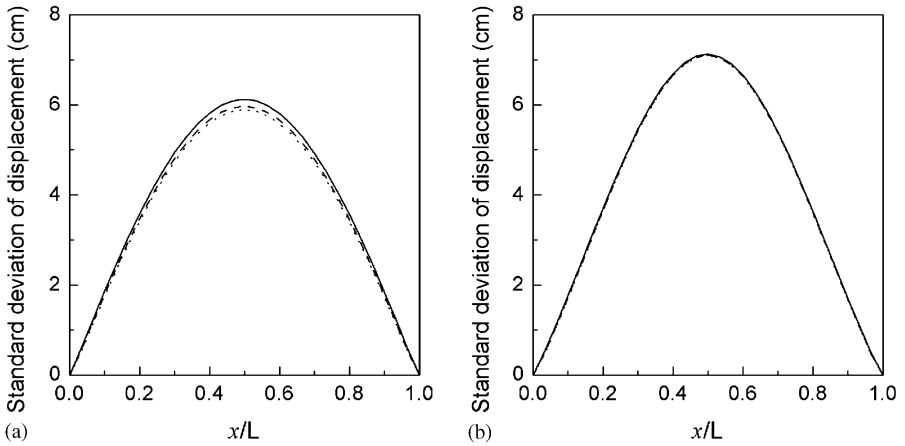

Fig. 6. Variation of the dynamic response of the cable with n: solid line, $n = 29$; dashed line, $n = 59$; dotted line, $n = 89$. (a) external force; (b) support point motion.

corresponding to the components is $F_y = F_z = 247.5\,\mathrm{N/m}$. The displacements of supporting points are set to zero.

Fig. 8 shows the displacement response history at the mid-span of the cable. Fig. 9 shows the standard deviation of the displacement of each node of the cable obtained by ergodic sampling. It is seen that both viscous dampers and MR dampers can effectively suppress the cable vibrations. Given that the stochastic excitation primarily causes vibrations in the first mode, and the viscous damper has been tuned to vibrations in this mode, it is expected that both the MR damper and the viscous damper will work well in this case. As is seen this is indeed the case. The MR damper is only performing slightly better than the optimal tuned viscous damper.

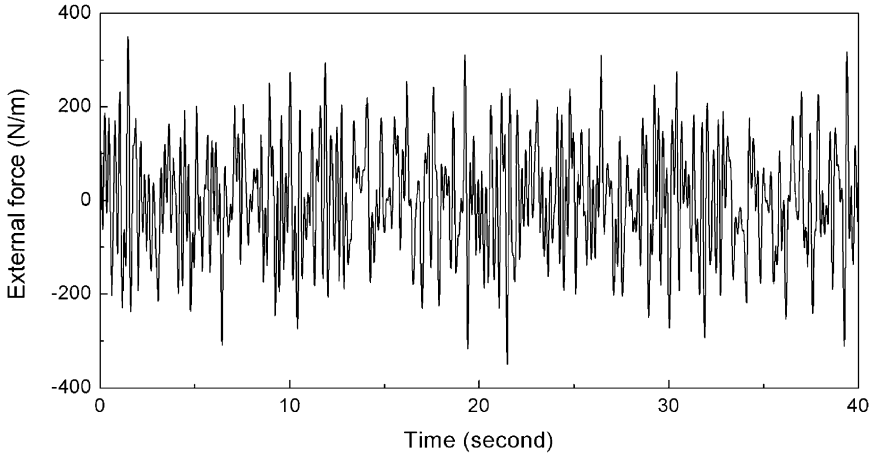

Fig. 7. Time history of uniformly distributed external force.

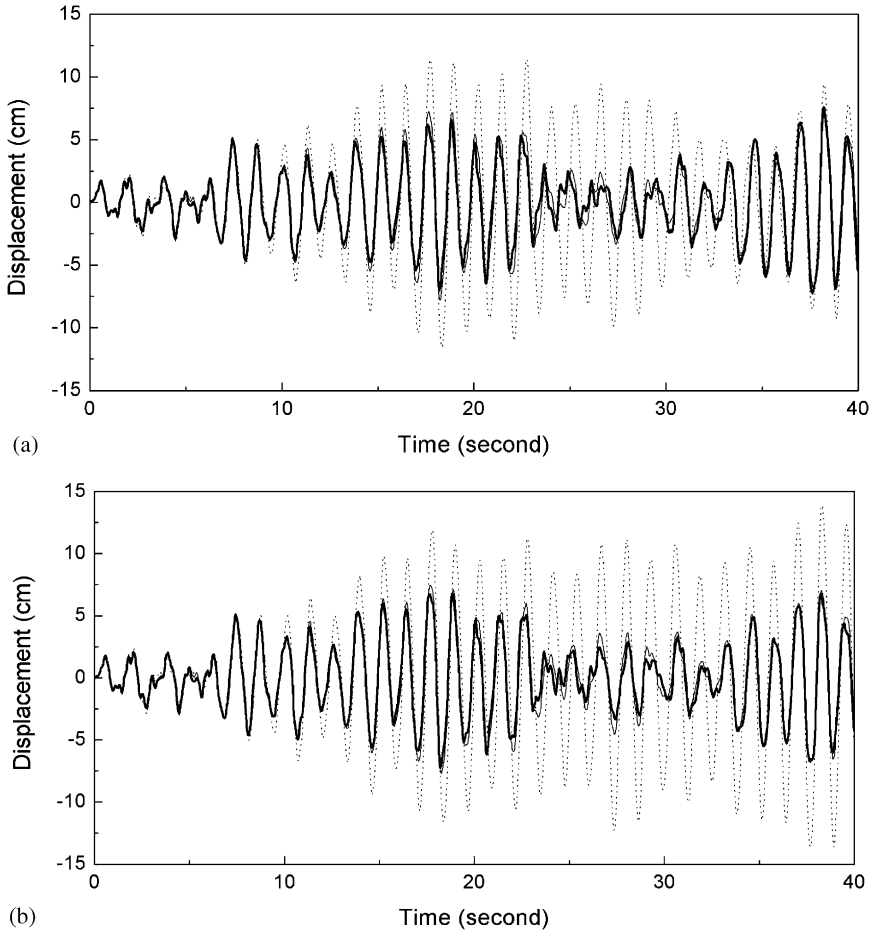

Fig. 8. Displacement response history at the mid-span of the cable: thick line, MR damper; thin line, viscous damper; dotted line, without damper. (a) in the Y direction; (b) in the Z direction.

It may be possible for one control strategy to decrease the motion significant in some regions of a cable but allow other parts to vibrate relatively unimpeded. Thus, the primary measure of damper performance is the mean square cable deflection integrated along the length of the cable,

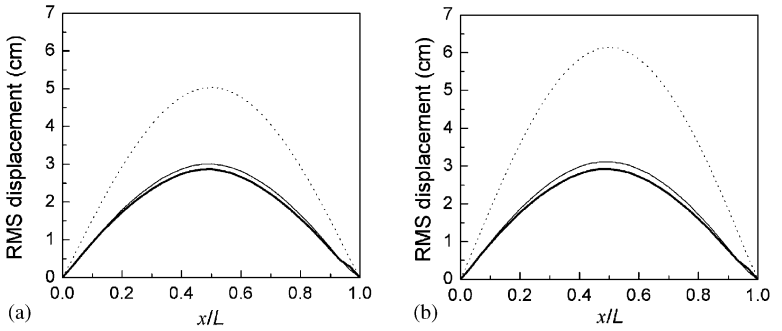

Fig. 9. Standard deviation of the displacement of each node of the cable: thick line, MR damper; thin line, viscous damper; dotted line, without damper. (a) in the Y direction; (b) in the Z direction.

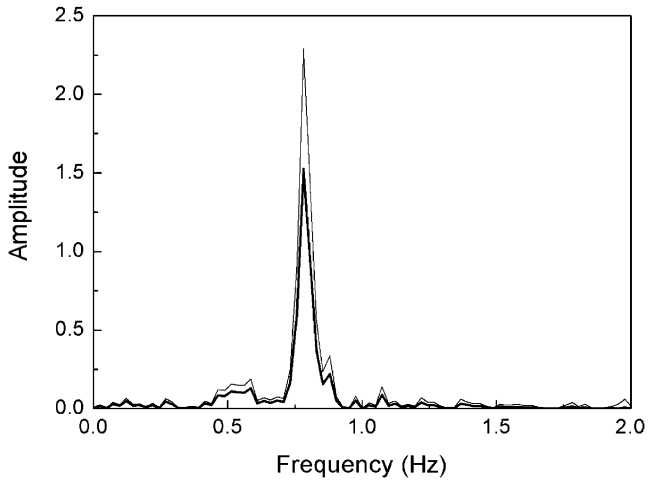

Fig. 10. Fourier spectrum of the displacement response of the cable without dampers: thick line, at the quarter-span; thin line, at the mid-span.

defined by [16]

$$\sigma_{\text{disp}}^2 = E\left[\int_0^l w^2(x,t)\,\mathrm{d}x\right]. \tag{39}$$

The displacement measure σ_{disp} of the cable without control, with viscous dampers and with MR dampers are 0.426, 0.252 and 0.240 $\text{m}^{3/2}$ in the Y direction, and 0.520, 0.262 and 0.245 $\text{m}^{3/2}$ in the Z direction, respectively. Therefore, MR dampers only provide 4.8% and 6.5% reduction of the cable response in the Y and Z direction compared to the optimal tuned viscous linear dampers with the proposed semi-active control algorithm. Fig. 10 shows the Fourier spectrum of the displacement response at the mid-span and at the quarter-span in the Y direction, respectively. It is seen that the peak value is located at 0.781 Hz, which is in the vicinity of the first in-plane natural frequency, indicating the predominating response in the first mode.

Figs. 11 and 12 illustrate the applied voltage history and relationship between control force and displacement of the MR dampers. Although these two MR dampers are installed symmetrically at the same node of the cable, the displacement and hence the control signal for each MR damper are different because the motion of the cable is three-dimensional (see Eqs. (21) and (23)). It is seen that the MR damper linking points C and E almost behaves like a passive nonlinear damper, and while, the MR damper linking points D and E serves as a smart damper whose applied maximum voltage is less than 3.5 V.

Next, in order to investigate the control effect of the cable during multimode vibrations, the cable is subjected to an in-plane concentrated harmonic excitation at a position of $0.2L$ near the damper. The

harmonic excitation is in the form

$$F = F_0[\chi \sin(2\pi f_1 t) + (1-\chi)\sin(2\pi f_2 t)], \tag{40}$$

where F_0 is the exciting force amplitude, f_1 and f_2 are the excitation frequencies, and χ is an interpolation parameter. In this example, the force amplitude F_0 is = 1300.0 N, the excitation frequencies f_1 and f_2 are taken to be 0.788 and 1.562 Hz, respectively, which are the first two natural frequencies of in-plane mode, and the interpolation parameter χ is 0.77. The displacement response history at the mid-span and at the quarter-span of the cable, and associated Fourier spectrum of cable without dampers are shown in Figs. 13 and 14, respectively. As we expected, the first two vibration modes are excited. The displacement measure σ_{disp} of the cable without control, with viscous dampers and with MR dampers are 0.279, 0.104 and 0.082 $\text{m}^{3/2}$ in the Y direction, respectively. Hence, MR dampers provide 21.2% reduction in cable response compared to the optimal tuned viscous linear dampers.

In conclusion, if two or more vibration modes of the cable are excited significantly, MR damper can achieve much better vibration reduction effect compared with viscous damper optimally tuned to a single of these modes.

4.2. Vibration from support point motion

Cables are always used as structural support element of masts, towers and cable-stayed bridges. The periodic motion of the cable supports is naturally associated with wind- or traffic-induced oscillations of the deck and/or the tower. If the frequency of oscillation of the deck or the tower falls in certain ranges, the cable may be excited and exhibit large response amplitudes. The most dangerous situations arise when the frequency of oscillation of some anchorage is in the neighbourhood of twice or equal to the first natural frequency of the

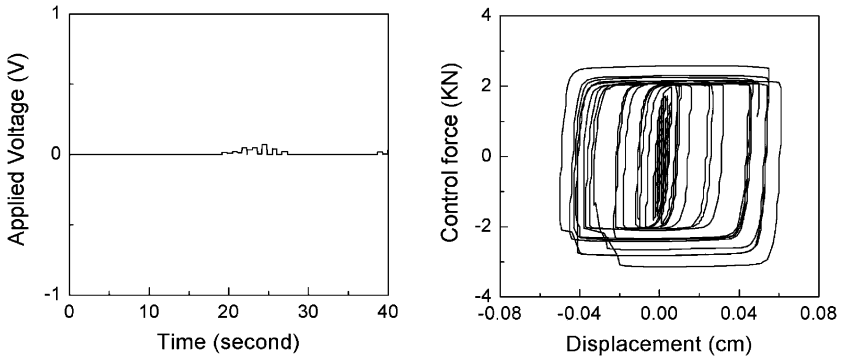

Fig. 11. Status of the MR damper linking point C and point E.

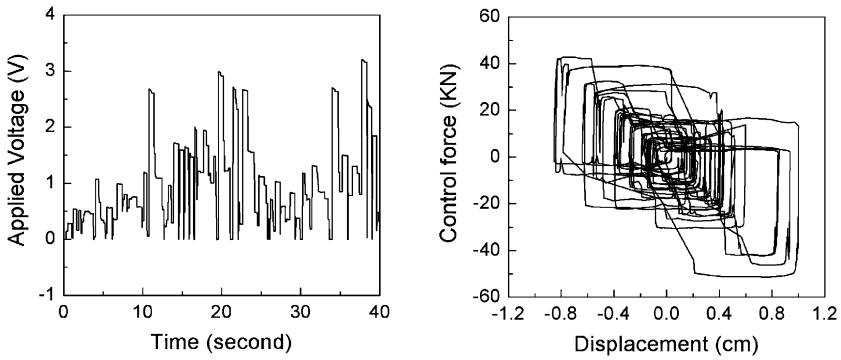

Fig. 12. Status of the MR damper linking point D and point E.

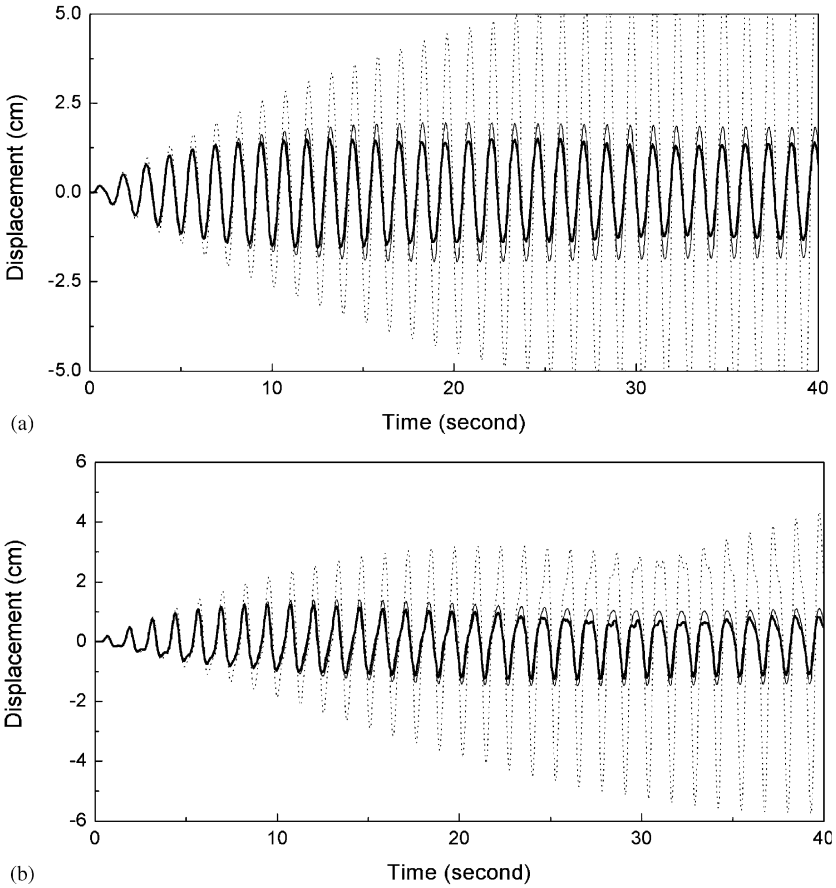

Fig. 13. Displacement response history of the cable subjected to the concentrated harmonic force: thick line, MR damper; thin line, viscous damper; dotted line, without damper. (a) displacement at the mid-span; (b) displacement at the quarter-span.

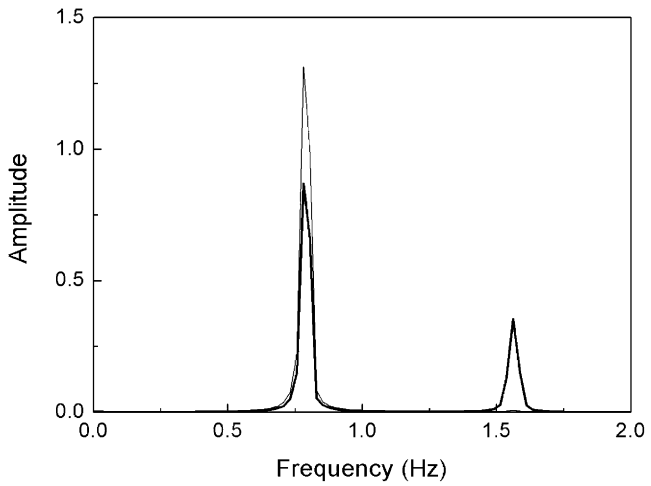

Fig. 14. Fourier spectrum of the displacement response of the cable without dampers: thick line, at the quarter-span; thin line, at the mid-span.

corresponding stay cable [37]. In this study, only the harmonic motion along the chord of the support B is considered, while the rest motions of support points are set to zero. The exciting force acting on the cable is ignored.

At first, the motion frequency Ω of the support B doubled the first natural frequency of in-plane mode, i.e. $\Omega = 1.576$ Hz, and the motion amplitude A is 0.045 m. Only in-plane vibration is induced by the motion of the support B. Fig. 15 shows the displacement history at the mid-span of the cable without dampers, with viscous dampers and with MR dampers, respectively. From Fig. 15, it can be seen that in the stationary range the maximum value reaches 1.31 m due to parametric resonance for the cable without dampers. The viscous damper can effectively mitigate vibration caused by parametric resonance. In the stationary range, the peak values are about 0.55 m. However, it can be found that the proper MR damper can prevent subharmonic vibration caused by the support point motion from taking place, and consequently can achieve quite good control effect. After the vibration of cable is stationary, the peak values are only about 0.04 m.

Then the motion amplitude of the support B increases to 0.06 m while the motion frequency is unchangeable. The displacement response at the mid-span of the cable with viscous dampers and with MR dampers is shown in Fig. 16. It can be found that, because the motion amplitude exceeds a certain threshold value, the subharmonic vibration occurs for the cable both with viscous dampers and MR dampers. Because the viscous damper is tuned to the first mode, the MR damper and viscous damper are performing similarly.

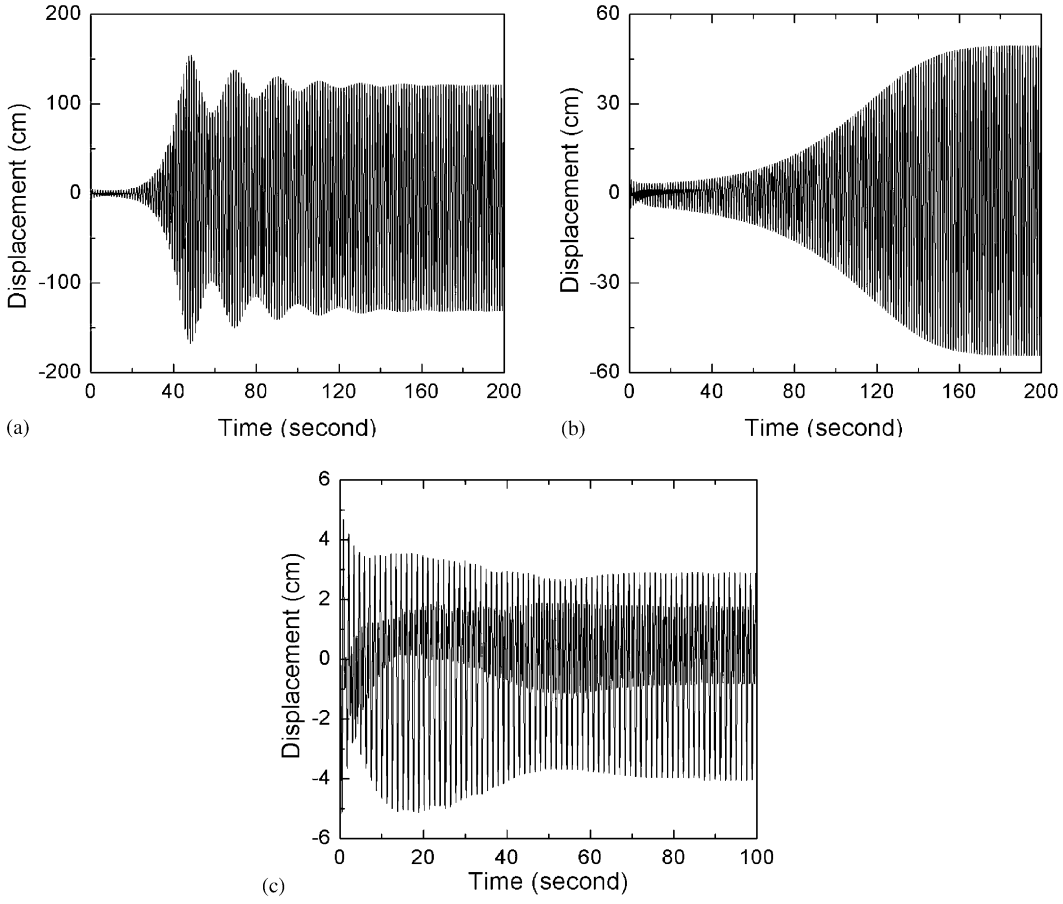

Fig. 15. Displacement response history at the mid-span of the cable caused by support point motion, $\Omega = 1.576$ Hz, $A = 0.045$ m: (a) without damper; (b) with viscous dampers; (c) with MR dampers.

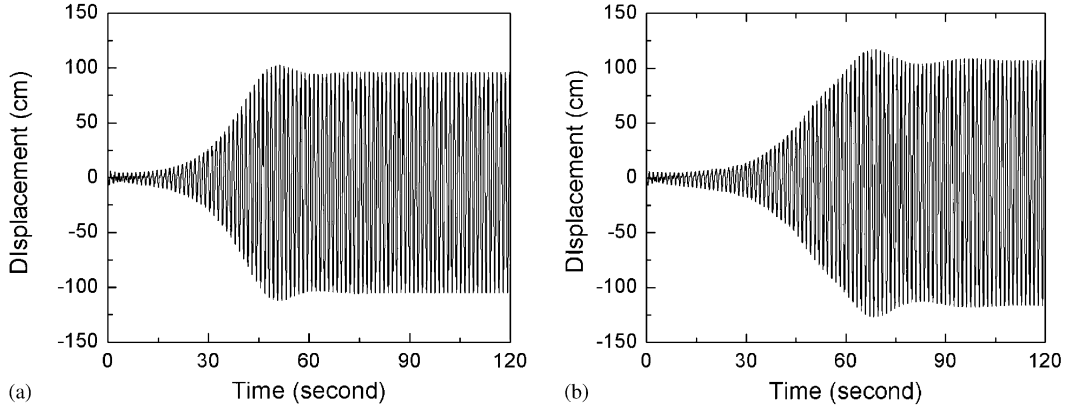

Fig. 16. Displacement response history at the mid-span of the cable caused by support point motion, $\Omega = 1.576$ Hz, $A = 0.06$ m: (a) with viscous dampers; (b) with MR dampers.

Next the motion frequency of the support B is set as the first natural frequency of in-plane mode, i.e. $\Omega = 0.788$ Hz, and the motion amplitude is still 0.045 m. Fig. 17 shows the displacement history at the mid-span of the cable without dampers, with viscous dampers and with MR dampers, respectively. In these three cases, it can be seen that cable oscillation excited by the motion of the support exhibits large amplitude responses. The peak values of displacement at the mid-span are 1.05 m (without dampers), 0.74 m (viscous dampers) and 0.67 m (MR dampers), respectively. Therefore, one can find again that both viscous damper and MR damper can suppress cable vibration significantly. Compared with viscous damper, MR damper can provide 9.4% reduction at the mid-span; in other words, MR damper can only provide a slight better vibration reduction effect.

4.3. Vibration from the combination of external force and support motion

In general, the dynamic response of the cable is induced by both the external force and support movement. The external force can be simulated by a broad-banded random process, while the support movement can be represented by a narrow-banded random process [38]. In practice, the most likely support excitation is not directly along the chord of the cable, for simplicity, only the motion along the chord of the support B is considered. The cable is subjected to a uniformly distributed random load described in Section 4.1. The peak value of the applied load is 350 N/m acting in the XY plane. The support movement is assumed to be harmonic motion, whose amplitude is 0.10 m. The motion frequency of the support is selected to be other values that cannot result in parametric resonance.

The dynamic response of the cable when the motion frequency Ω of the support B is 1.0 and 1.48 Hz are shown in Figs. 18 and 19, respectively. From Fig. 18, it can be seen that, when Ω is 1.0 Hz, which is close to the first natural frequency of the cable, the dynamic responses of cable with viscous damper and with MR damper are very close. The displacement measures σ_{disp} of the cable with viscous damper and with MR damper are 1.458 and 1.454 $\text{m}^{3/2}$, respectively. The σ_{disp} ratio of the latter to the former is 0.997. From Fig. 19, one can find that, when Ω is 1.48 Hz, which is close to the second natural frequency of the cable, MR damper can achieve better control effect than viscous damper does. The displacement measures σ_{disp} of the cable with viscous damper and with MR damper are 1.360 and 0.988 $\text{m}^{3/2}$, respectively. Then the σ_{disp} ratio of the latter to the former is 0.726, in other words, the MR damper provides about 27% reduction compared to the viscous damper. A possible explanation about this is that, as mentioned in Section 4.1, when cable subjected to the combination of the uniformly distributed broad-banded random external force and the supportly movement, if the motion frequency Ω of the support is about equal to the second natural frequency of the cable, the first two vibration modes are excited, so MR damper can more effectively mitigate dynamic response of the cable compared to viscous damper; and while, if Ω is close to the first natural frequency of the cable, only the first vibration mode is excited, so the vibration reduction effect provided by MR damper and by viscous damper is similar.

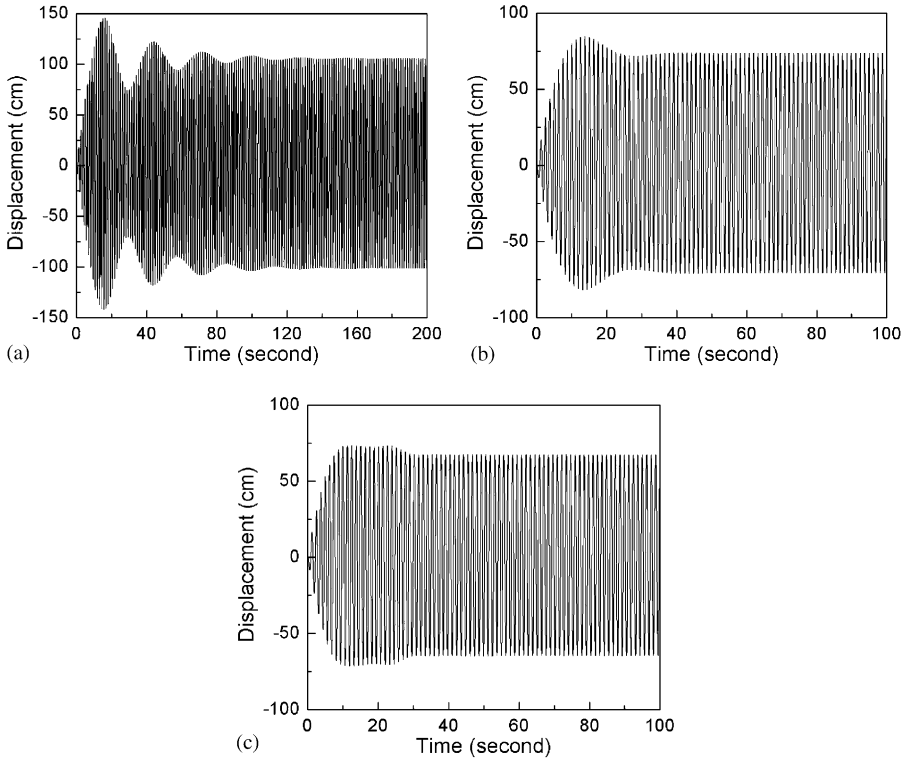

Fig. 17. Displacement response history at the mid-span of the cable caused by support point motion, $\Omega = 0.788$ Hz, $A = 0.045$ m: (a) without damper; (b) with viscous dampers; (c) with MR dampers.

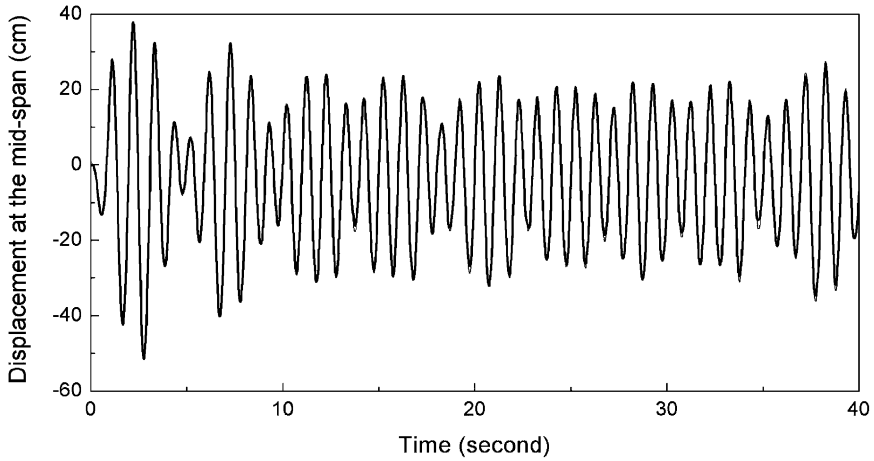

Fig. 18. Displacement response history of the cable, $\Omega = 1.0$ Hz, $A = 0.10$ m: thick line, MR damper; thin line, viscous damper.

4.4. Influence of controller gain β

Controller gain β plays an important role in semi-active control rule, and should be selected carefully. Fig. 20 shows the variations of the displacement measure σ_{disp} of the cable with the controller gain. It is seen that there exists an optimal β by which the best performance of the MR dampers can be achieved. This may be because that if β is selected too small or too large, the applied voltage would keep constant (0 or $V_{\max}$), that is,

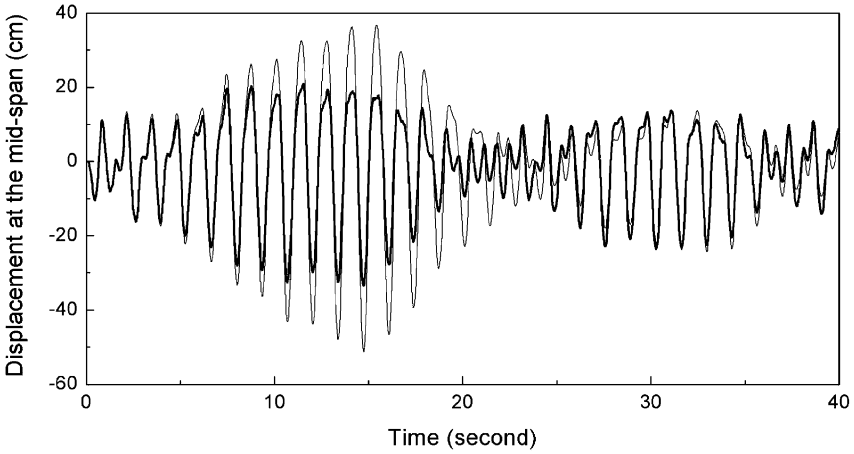

Fig. 19. Displacement response history of the cable, $\Omega = 1.48$ Hz, $A = 0.10$ m: thick line, MR damper; thin line, viscous damper.

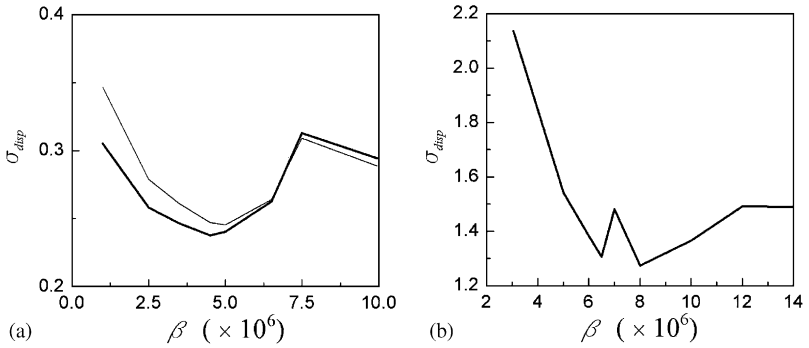

Fig. 20. Variations of the displacement measure σ_{disp} with the controller gain: thick line, in the Y direction; thin line, in the Z direction. (a) uniform distributed force; (b) combination of external force and the support motion.

the semi-active damper is served as the passive damper, then the property of the damper cannot be modulated according to the cable vibration and consequently the best vibration reduction effect cannot be obtained. Fig. 20 shows that the σ_{disp} can be reduced from 0.426 (without control) to 0.237 $\text{m}^{3/2}$ in the Y direction and from 0.520 (without control) to 0.247 $\text{m}^{3/2}$ in the Z direction in the case of uniformly distributed random external force, while the σ_{disp} can be reduced from 4.201 (without control) to 1.274 $\text{m}^{3/2}$ when the cable is subjected to the combination of random external force and the support point harmonic motion, whose amplitude is 0.16 m and frequency is 1.4 Hz, respectively, if the optimal β is selected. However, under different situations, the optimal β is different. Therefore, a trade-off controller gain β should be selected prudently only after comprehensive studies under different loading conditions, including external force and motion of support point and others.

4.5. Robustness of the control algorithm

In practice, the structural parameters can hardly be obtained accurately, so it is important that the control algorithm is robust. The implementation of the adopted control strategy only requires the displacement and velocity of MR dampers, and only the rough estimation on the structural parameters of the cable is required. Hence, it is suitable for the structures whose parameters are inaccurate. After rough estimation on structural

parameters and selection of a proper β, an appropriate semi-active control scheme can be obtained. On the basis of this, even the selection of structural parameters deviate from the true ones, the better control effect can still be achieved. In this study, the ratio of true equilibrium force H^* to the estimated force H is assumed to be variable from 0.85 to 1.10. Fig. 21 shows the variations of the displacement measure σ_{disp} of cable with H^*/H when the cable is subjected to the uniformly distributed random force. The vibration of the cable with viscous damper is also demonstrated in order to verify the robustness and effectiveness of the control algorithm. It is seen that MR damper can provide better vibration reduction effect than that by viscous damper in the given range of H^*/H.

4.6. Influence of measurement noise

In general, displacement signals are generated through integrated velocity or acceleration signals by hardware, which results in the error of displacement inevitably. The applied voltage to MR dampers is determined by local peak of displacement, so it is necessary to study the influence of measurement noise level. Fig. 22 shows the variations of the displacement measure σ_{disp} of cable with measurement noise level ζ when the cable is subjected to the concentrated harmonic force. It is seen that, with the increase of the ζ, the σ_{disp} increases from 0.0823 to 0.09 $\mathrm{m}^{3/2}$, that is, the performance of MR damper decreases. Therefore, the measurement error of displacement should be made as small as possible. However, the decrease of

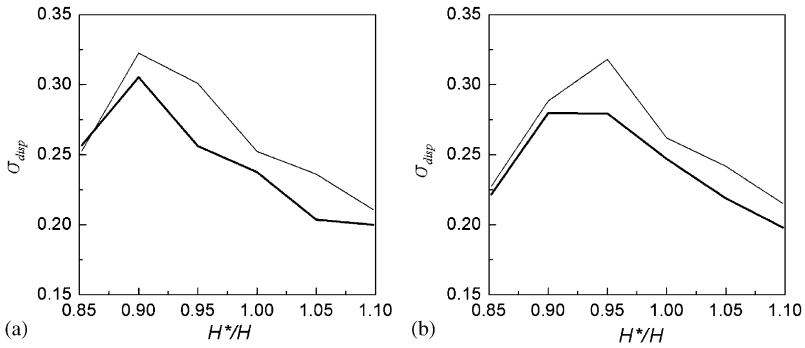

Fig. 21. Variations of the displacement measure σ_{disp} with H^*/H when the cable is subjected to the uniform distributed random force: thick line, MR damper; thin line, viscous damper. (a) in the Y direction; (b) in the Z direction.

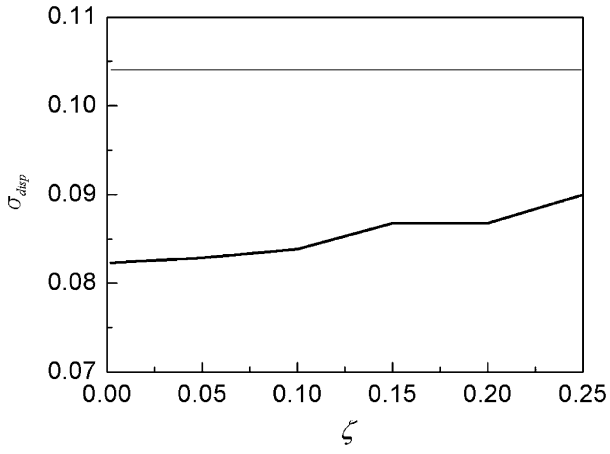

Fig. 22. Variations of the displacement measure σ_{disp} with measurement noise level ζ when the cable is subjected to the concentrated harmonic force: thick line, MR damper; thin line, viscous damper.

performance of MR is less than 10% and the control effect by MR dampers is still better than that by viscous damper. So the influence of measurement noise on vibration reduction effect is not significant using semi-active control strategy based on the modulated homogeneous friction algorithm.

5. Conclusions

A formulation for three-dimensional nonlinear semi-active vibration control of an inclined sag cable installed with MR dampers has been presented in this paper. A modified Dahl model is used to describe the dynamic property of MR damper. The nonlinear equations of motion of the cable–damper system are proposed, taking the cable sag, cable inclination, bending stiffness of the cable, damper direction and others into consideration. The derived governing equations account for coupling between in-plane and out-of-plane motions, and also for the displacement of the support points. Essentially, MR damper can be considered as a variable friction damper, so a semi-active control rule based on the modulated homogeneous friction algorithm is proposed. Because only the local dynamic response of MR dampers should be required, and the structural parameters of the cable can be inaccurate, the proposed control rule is easily implemented and robust.

Taking a typical short cable as an example, the vibration reduction ability with MR dampers is verified by comparison with the optimal viscous damper. The numerical results show that, when the proposed semi-active control strategy based on the modulated homogeneous friction algorithm is adopted, if only one vibration mode of cable is excited, the vibration reduction effect by MR damper is close to that by viscous damper optimally tuned to this mode; however, if two or more vibration modes of cable are excited, MR damper can achieve better vibration reduction effect compared with viscous damper. In addition, when the motion frequency along the chord of the support point is in the neighbourhood of two times the first natural frequency of the corresponding cable, if the amplitude of the support point motion less than a threshold value, MR damper can prevent the evolution of subharmonic excitation while viscous damper cannot, consequently, MR damper can significantly mitigate the vibration of the cable; however, when the motion frequency of support points is in the neighbourhood of the first natural frequency of the cable, the parametric resonance cannot be avoided and the vibration reduction effect by MR damper and by viscous damper is similar.

In order to realize the proposed control scheme, only controller gain should be determined. However, in different situations, the optimal value of controller gain is different. Therefore, a trade-off controller gain should be selected carefully only after comprehensive studies under various loading conditions. Through altering structural parameters, the robustness of the control rule is verified. In addition, although the increase of measurement noise level will lead to decrease in the control effect, the reduced degree is slight. So it can be believed that the influence of measurement noise on vibration reduction effect is unimportant.

Acknowledgements

The first writer is grateful for the financial support from the Chenguang Project of Wuhan City under Grant 20025001031 and a visiting appointment at the Aalborg University, Denmark. The suggestions provided by the anonymous referees are also appreciated.

References

[1] S.C. Watson, D. Stafford, Cables in trouble, *Civil Engineering, ASCE* 58 (1988) 38–41.
[2] I. Kovacs, Zur frage der Seilschwingungen und der Seildampfung, *Die Bautechnik* 59 (1981) 325–332 (in German).
[3] B.M. Pacheo, Y. Fujino, A. Sulekh, Estimation curve for modal damping in stay cables with viscous damper, *Journal of Structural Engineering, ASCE* 119 (1993) 1961–1979.
[4] Z. Yu, Y.L. Xu, Mitigation of three-dimensional vibration of inclined sag cable using discrete oil dampers. I. Formulation, *Journal of Sound and Vibration* 214 (1998) 659–673.
[5] S. Krenk, Vibrations of a taut cable with an external damper, *Journal of Applied Mechanics* 67 (2000) 772–776.
[6] S. Krenk, S.R.K. Nielsen, Vibrations of a shallow cable with a viscous damper, *Proceedings of the Royal Society, London A* 458 (2002) 339–357.

[7] S.R.K. Nielsen, S. Krenk, Whirling motion of a shallow cable with viscous dampers, *Journal of Sound and Vibration* 265 (2003) 417–435.
[8] J.A. Main, N.P. Jones, Free vibrations of taut cable with attached damper. I: linear viscous damper, *Journal of Engineering Mechanics, ASCE* 128 (2002) 1062–1071.
[9] T.G. Carne, Guy cable design and damping for vertical axis wind turbines, Report No. SAN80-2669, Sandia National Laboratories, Albuquerque, NM, 1981.
[10] I. Kovacs, E. Strommen, E. Hjorth-Hansen, Damping devices against cable oscillations on Sunningesund Bridge, *Proceedings of the Third International Symposium on Cable Dynamics*, AIM, Liege, Belgium, 1999, pp. 145–150.
[11] J.A. Main, N.P. Jones, Free vibrations of taut cable with attached damper. II: nonlinear damper, *Journal of Engineering Mechanics, ASCE* 128 (2002) 1072–1081.
[12] T. Susupow, Y. Fujino, Active control of multimodal cable vibrations by axial support motion, *Journal of Engineering Mechanics, ASCE* 121 (1995) 964–972.
[13] Y. Achkire, Active Tendon Control of Cable-Stayed Bridges, PhD Thesis, ULB, Belgium, 1997.
[14] A. Preumont, F. Bossens, Active tendon control of cable-stayed bridges: a large-scale demonstration, *Earthquake Engineering and Structural Dynamics* 30 (2001) 961–979.
[15] B. Xu, Z.S. Wu, K. Yokoyama, Neural networks for decentralized control of cable-stayed bridge, *Journal of Bridge Engineering, ASCE* 8 (2003) 229–236.
[16] E.A. Johnson, R.E. Christenson, B.F. Spencer Jr., Semiactive damping of cables with sag, *Computer Aided Civil and Infrastructure Engineering* 18 (2003) 132–146.
[17] Y.Q. Ni, Y. Chen, J.M. Ko, D.Q. Cao, Neuro-control of cable vibration using semi-active magneto-rheological dampers, *Engineering Structures* 24 (2002) 295–307.
[18] S.J. Moon, L.A. Bergman, P.G. Voulgaris, Sliding mode control of cable-stayed bridge subjected to seismic excitation, *Journal of Engineering Mechanics, ASCE* 129 (2003) 71–78.
[19] Y.Q. Ni, J.M. Ko, Z.Q. Chen, B.F. Spencer Jr., Lessons learned from application of semiactive MR dampers to bridge cables for wind-rain-induced vibration control, *China–Japan Workshop on Vibration Control and Health Monitoring of Structures and Third Chinese Symposium on Structural Vibration Control*, Shanghai, China, 2002.
[20] Z.Q. Chen, X.Y. Wang, Y.Q. Ni, J.M. Ko, Field measurements on wind-rain-induced vibration of bridge cables with and without MR dampers, *The Third World Conference on Structural Control*, Como, Italy, 2002.
[21] A.B. Mehrabi, H. Tabatabai, Unified finite difference formulation for free vibration of cables, *Journal of Structural Engineering, ASCE* 124 (1998) 1313–1322.
[22] C.G. Koh, Y. Rong, Dynamic analysis of large displacement cable motion with experimental verification, *Journal of Sound and Vibration* 272 (2004) 187–206.
[23] Y.Q. Ni, W.J. Lou, J.M. Ko, A hybrid pseudo-force/Laplace transform method for non-linear transient response of a suspended cable, *Journal of Sound and Vibration* 238 (2000) 189–214.
[24] P.D. Gosling, E.A. Korban, A bendable finite element for the analysis of flexible cable structures, *Finite Element in Analysis and Design* 38 (2001) 45–63.
[25] B.F. Spencer Jr., S.J. Dyke, M.K. Sain, J.D. Carlson, Phenomenological model for magnetorheological damper, *Journal of Engineering Mechanics, ASCE* 123 (1997) 230–238.
[26] Q. Zhou, W.L. Qu, Two mechanical models for magnetorheological damper and corresponding test verification, *Earthquake Engineering and Engineering Vibration* 22 (2002) 144–150 (in Chinese).
[27] P.R. Dahl, Solid friction damping of mechanical vibrations, *AIAA Journal* 14 (1976) 1675–1682.
[28] H.M. Irvine, *Cable Structures*, MIT Press, Cambridge, MA, 1981.
[29] P. Warnitchai, Y. Fujino, T. Susumpow, A non-linear dynamic model for cables and its application to a cable-structure system, *Journal of Sound and Vibration* 187 (1995) 695–712.
[30] G.V. Rao, R.N. Iyengar, Seismic response of a long span cable, *Earthquake Engineering and Structural Dynamics* 20 (1991) 243–258.
[31] M. El-Attar, A. Ghobarah, T.S. Aziz, Non-linear cable response to multiple support periodic excitation, *Engineering Structures* 22 (2000) 1301–1312.
[32] K.J. Bathe, *Finite Element Procedures in Engineering Analysis*, Prentice-Hall, Englewood Cliffs, NJ, 1982.
[33] J.A. Inaudi, Modulated homogeneous friction: a semi-active damping strategy, *Earthquake Engineering and Structural Dynamics* 26 (1997) 361–376.
[34] T.T. Soong, *Active Structure Control: Theory and Practice*, Longman Scientific & Technical, New York, 1990.
[35] N.B. Kahla, Dynamics of a single guy cable, *Computers and Structures* 54 (1995) 1197–1211.
[36] Y.L. Xu, Z. Yu, Mitigation of three-dimensional vibration of inclined sag cable using discrete oil dampers. II: application, *Journal of Sound and Vibration* 214 (1998) 675–693.
[37] A. Pinto da Costa, J.A.C. Martins, F. Branco, J.L. Lilien, Oscillations of bridge stay cables induced by periodic motions of deck and/or tower, *Journal of Engineering Mechanics, ASCE* 122 (1996) 613–622.
[38] J.W. Larsen, S.R.K. Nielsen, Nonlinear stochastic response of a shallow cable, *International Journal of Non-linear Mechanics* 41 (2006) 327–344.